OXFORD

Cerebral Cortex, 2016, 1–17

doi: 10.1093/cercor/bhw139
Original Article

ORIGINAL ARTICLE

Reconfiguration of Intrinsic Functional Coupling Patterns Following Circumscribed Network Lesions

Mark C. Eldaief[1,2,3], Stephanie McMains[1], R. Matthew Hutchison[1], Mark A. Halko[3] and Alvaro Pascual-Leone[3,4]

[1]Center for Brain Science Neuroimaging Facility, Harvard University, Cambridge, MA 02138, USA, [2]Division of Cognitive and Behavioral Neurology, Department of Neurology, Brigham and Women's Hospital, Harvard Medical School, Boston, MA 02115, USA, [3]Berenson-Allen Center for Noninvasive Brain Stimulation, Department of Neurology, Division of Cognitive Neurology, Beth Israel Deaconess Medical Center, Harvard Medical School, Boston, MA 02215, USA and [4]Institut Guttmann, Universitat Autonoma, Barcelona, Spain

Address correspondence to Mark C. Eldaief, Harvard University Center for Brain Sciences, Northwest Building, 52 Oxford Street, Cambridge, MA 02138, USA; Brigham and Women's Hospital, 221 Longwood Avenue, Boston, MA 02115, USA. Email: meldiaef@partners.org

Abstract

Communication between cortical regions is necessary for optimal cognitive processing. Functional relationships between cortical regions can be inferred through measurements of temporal synchrony in spontaneous activity patterns. These relationships can be further elaborated by surveying effects of cortical lesions upon inter-regional connectivity. Lesions to cortical hubs and heteromodal association regions are expected to induce distributed connectivity changes and higher-order cognitive deficits, yet their functional consequences remain relatively unexplored. Here, we used resting-state fMRI to investigate intrinsic functional connectivity (FC) and graph theoretical metrics in 12 patients with circumscribed lesions of the medial prefrontal cortex (mPFC) portion of the Default Network (DN), and compared these metrics with those observed in healthy matched comparison participants and a sample of 1139 healthy individuals. Despite significant mPFC destruction, patients did *not* demonstrate weakened intrinsic FC among undamaged DN nodes. Instead, network-specific changes were manifested as weaker negative correlations between the DN and attentional and somatomotor networks. These findings conflict with the DN being a homogenous system functionally anchored at mPFC. Rather, they implicate a role for mPFC in mediating cross-network functional interactions. More broadly, our data suggest that lesions to association cortical hubs might induce clinical deficits by disrupting communication between interacting large-scale systems.

Key words: default network, intrinsic functional connectivity, lesion, mPFC, negative correlations

Introduction

Successful information processing is dependent on communication across distributed brain regions. Functional relationships among cortical regions have been inferred on the basis of the relative strength of intrinsic functional connectivity (FC) between them, as revealed by various fMRI imaging approaches (Biswal et al. 1995; Beckmann et al. 2005). Through such methods, distinct large-scale functional brain networks have been reliably characterized (Damoiseaux et al. 2006; Power et al. 2011; Yeo et al. 2011).

Network functional relationships can be further delineated through causal perturbations of individual network regions (Eldaief et al. 2011). One strategy is to gauge the effects of circumscribed lesions to network regions (or nodes) (Kaiser et al. 2007; Bullmore and Sporns 2009; Gillebert and Mantini 2013). Lesion effects have consistently been shown to occur among distal and undamaged network regions, consistent with the phenomenon

of "functional diaschisis" (Silasi and Murphy 2014). Several studies of human lesions have emphasized that distal intrinsic FC effects of focal lesions respect the boundaries of the network affected (Carter et al. 2010; Nomura et al. 2010; van Meer et al. 2010; Wang et al. 2010). Similarly, behavioral consequences of discrete lesions can be understood on the basis of the broader cortical network to which the lesioned cortex is affiliated (He et al. 2007; Boes et al. 2015).

However, far fewer studies have focused on the effects of circumscribed lesions upon more global intrinsic FC relationships; for example, those across cortical systems. Despite this, "higher-order" cognitive processing (e.g. mental flexibility, reasoning, executive function) is likely to depend on such intrinsic functional interactions (Kelly et al. 2008; Boveroux et al. 2010; Hampson et al. 2010; Barber et al. 2013; Chai et al. 2014). One such avenue of exploration is to examine the intrinsic FC impact of lesions to heteromodal association cortex in general, or to hub regions in particular. Hubs are cortical regions whose diverse connectivity profile and/or functional positioning facilitate information integration across diverse inputs (Buckner et al. 2009; Power et al. 2013). Hubs can be differentially characterized by different graph theoretical metrics, leading to some disagreement as to which regions most accurately represent hubs for global cortical processing. For example, Power et al. (2013) used participation coefficients as well as the identification of regions wherein multiple functional systems are represented (high system density) to identify cortical hubs. Here, we define hubs as nodes exhibiting high degree and high centrality (Bullmore and Sporns 2009).

Evidence for global FC aberrations in the setting of hub destruction has come in the form of computational modeling studies based on macaque (Honey and Sporns 2008) and human (Alstott et al. 2009) structural connectivity datasets. Gratton et al. (2012) demonstrated decreased global cortical modularity in the setting of damage to regions with high participation coefficients, and this was even observed in the nonlesioned hemisphere. Moreover, Warren et al. (2014) demonstrated profound and varied neuropsychological deficits in the setting of damage to different cortical hubs (identified with participation coefficient and system density metrics). Taken together, lesions to heteromodal association cortex may be expected to induce intrinsic FC aberrations which extend beyond the network to which said region is affiliated, particularly, if the damage involves a global cortical hub.

Motivated by such considerations, we investigated how circumscribed lesions of the default network (DN) would impact intra- and internetwork intrinsic functional relationships. The DN is large-scale cortical network comprised of interacting heteromodal association regions. It is also arguably the most well-characterized intrinsic FC network, with within-network connectivity being reproducible across scanning paradigms and analytic approaches (Shehzad et al. 2009). Furthermore, the DN exhibits topographically specific and reproducible functional relationships with attentional and somatosensory cortical systems in the form of negative correlations (or "anticorrelations") (Fox et al. 2005). This raises the question of whether DN damage could indirectly affect functional cohesion within these systems, or between them and the DN. Lastly, two of the network's major nodes, the posterior cingulate/ventral precuneus (pCC) and the medial prefrontal cortex (mPFC), have been assigned as DN hubs (Fransson and Marrelec 2008; Gao et al. 2009; Andrews-Hanna et al. 2010), as well as global cortical hubs (Alstott et al. 2009; Buckner et al. 2009; Cole et al. 2010; Sepulcre et al. 2010). As such, lesions involving these cortical midline structures could have far reaching functional consequences.

We measured intrinsic FC with resting-state functional MRI (rs-fMRI) via a seed-based approach. We examined changes in region-to-region intrinsic FC, as well as graph theoretical metrics assessing nodal hub properties (degree and centrality), in patients with stable and circumscribed cortical lesions of mPFC, and compared these metrics with those obtained from one-to-one matched healthy comparison participants and a large dataset ($n = 1139$) of healthy individuals made available through an open source database (Holmes et al. 2015). We predicted that because mPFC has been characterized as a DN hub, mPFC lesions would induce distributed changes among undamaged DN nodes (e.g. between pCC and posterior inferior parietal cortex [pIPL]). However, we also predicted that mPFC damage would impact other intrinsic FC networks and/or affect internetwork couplings, in light of its classification as association cortex and as a putative global hub. While it is well recognized that lesions induce cognitive deficits through distal effects within the network affected (Corbetta 2012), the latter finding would raise the novel possibility that there is a cross-network basis for certain cognitive deficits following circumscribed brain injury.

Materials and Methods

Lesion Selection and Participants

Twelve right-handed patients with chronic and stable mPFC lesions participated in the study. Of note, whereas the posterior cingulate/ventral precuneus (pCC) is often described as the predominant DN hub, the relative scarcity of pCC lesions (Leech et al. 2012) led to the choice of studying mPFC lesion patients. Patient demographics and lesion etiology are shown in Table 1. While no age exclusions were employed in patient selection, the patient participants discovered were relatively young (mean age = 38.2, SD = 13.8, range 23–64, 6 females), which allowed us to minimize confounding effects of advanced age upon intrinsic FC (Andrews-Hanna et al. 2007). Neuropsychological metrics were not formally assessed as part of this study. However, certain cognitive assessments were taken as part of the patients' medical care and these are presented in Supplementary Table 1. Patients 1, 3, and 6 (and to a lesser extent patient 9) exhibited significant abulia, which is a common sequela of significant mPFC injury (Devinsky et al. 1995; Stuss 2011). Expectedly, other neuropsychological deficits in patients tended to involve frontal-subcortical domains such as working memory or processing speed. All patients were ambulatory, not aphasic and without gross motor or sensory deficits on elemental neurological examinations. Nine out of the 12 patients were completely functionally independent. Patients 1, 3, and 6 had varying degrees of functional dependence. Patient 4 carried a distant diagnosis of mild bipolar affective disorder, but was psychiatrically stable at the time of participation. No other patient had a history of antecedent neurological or psychiatric history prior to their injury. Five out of the 12 patients were not on any central nervous system acting medications. Three out of the 12 patients were only on the antiepileptic medication levetiracetam used to treat, or as prophylaxis against, seizures resulting from their lesion. One other patient (Patient 4) was only on a benzodiazepine nightly. Another patient was only maintained on a single selective serotonin reuptake inhibitor (SSRI). The remaining two patients were on multiple centrally acting medications (Table 1).

We were particularly interested in recruiting participants with *large* mPFC lesions given that the mPFC portion of the DN is itself large, and that smaller lesions might not be expected to appreciably impact intrinsic FC. Lesion etiology included ischemic

Table 1 Demographics of patient participants

Patient number	Gender	Age	Education (years)	Time since injury (months)	Lesion etiology	Side affected	% destruction mPFC node[a]	% destruction entire DN	CNS medications at time of scanning
P1	M	29	16	16	SAH	Bilateral	65	27	S, S, AED**, AED, AD
P2	F	23	16	11	TBI	R > L	44	22	None
P3	F	60	12	5	SAH	Bilateral	46	20	AED**
P4	F	40	12	5	Mass lesion (meningioma)	Bilateral	43	19	BZ
P5	M	26	16	70	Mass lesion (neuroglial tumor)	Left	25	10	AED**
P6	F	52	14	34	Mass lesion (meningioma)	Bilateral	18	9	BZ, AED, AED, AP, AD
P7	M	35	10	9	Mass lesion (granuloma)	Bilateral	15	7	None
P8	M	24	Unknown	36	TBI	Bilateral	9	6	None
P9	M	64	12	5	TBI	Bilateral	11	5	AD
P10	F	41	14	5	SAH	Right	11	4	None
P11	M	33	12	24	SAH	Bilateral	5	2	None
P12	F	31	16	32	Mass lesion (dermoid cyst)	Left	4	2	AED**

SAH, subarachnoid hemorrhage; TBI, traumatic brain injury; S, stimulant; AED, antiepileptic drug; AED**, levetiracetam; AD, antidepressant; AP, atypical antipsychotic; BZ, benzodiazepine.

[a]Percent destruction mPFC node does not include damage to ventrolateral prefrontal cortex a part of the DN.

damage resulting from subarachnoid hemorrhage from rupture of an anterior communicating artery aneurysm ($n = 4$, two of whom suffered additional ischemic injury from anterior cerebral artery vasospasm); encephalomalacia resulting from traumatic brain injury ($n = 3$); and surgical resection of mass lesions ($n = 5$). Etiology of mass lesions included olfactory groove meningiomas (2/5, Patients 4 and 6), a benign dermoid cyst (1/5, Patient 12), and a large frontal granuloma (1/5, Patient 7). The remaining mass lesion patient (Patient 5) had an intermediate grade (World Health Organization [WHO] Grade II–III) tumor and had undergone two surgical resections (in the same surgical cavity, the second resection occurring 70 months prior to participation), as well as focal (but not whole brain) radiation (completed 30 months prior to participation). While the patient suffered a tumor recurrence 18 months following his participation, at the time of participation he was clinically stable (considered in remission) and his concurrent clinical MRI showed no evidence of residual tumor.

Heterogeneous lesion etiologies such as these have been employed in other human protocols examining intrinsic FC changes. For example, Warren et al. (2014) studied patients with benign meningioma resections as well as strokes. Other groups (Nomura et al. 2010; Gratton et al. 2012) studied patients with these lesion etiologies as well as patients with severe traumatic brain injury, mirroring the three lesion etiologies we examined. All lesions were restricted to frontal cortex (and adjacent subcortical white matter, but sparing subcortical gray matter). At the time of scanning, all patients were at least 5 months removed from their injury. Lesion duration was defined as the time between the patient's original injury (in the case of subarachnoid hemorrhage and TBI patients) and study participation. For patients with mass lesions, this was defined as the time between their surgical resection (in the case of Patient 5 his second resection) and study participation. All patients suffered a single neurological injury of the specified type, and no patient suffered an additional neurological injury during the period between their defined lesion acquisition and scanning. The mean lesion duration was 21 months (SD = 19.6, range 5–70). Therefore, all patients were considered as being in the chronic phase of cortical reorganization (Di Pino et al. 2014; Warren et al. 2014).

These 12 patients were one-to-one age and gender matched with 12 right-handed healthy comparison participants (mean age = 37.2, SD = 16.0, range 24–68) ($P = 0.87$), who had no neurological or psychiatric history. This group is henceforth referred to as the comparison group. Data from 7/12 comparison participants were taken from a concurrently running protocol. We employed this relatively small sample as our main comparison group because these participants underwent identical scanning parameters on the same scanner during the same time period as the patient group. However, in order to render our findings more generalizable, we also studied a much larger dataset. Data from 1139 healthy participants were obtained through an open source database (http://neuroinformatics.harvard.edu/gsp) (Holmes et al. 2015). To facilitate comparisons with our study protocol, we selected every subject within this database who had two (as opposed to one) functional runs-resulting in a total of 1139 participants.

All local participants provided written informed consent in accordance with the guidelines of the Committee on Clinical Investigations at the Beth Israel Deaconess Medical Center. One patient participant (Patient 1) provided written informed consent through a designated proxy.

Image Acquisition

All MR imaging was conducted at the Center for Biomedical Imaging, at Boston University Medical Center. MRI data were acquired using a 3.0-T whole-body scanner (Phillips™), equipped for echo-planar imaging with a 12-channel 3-axis gradient head coil. Head movements were restricted using foam cushions. Structural images were acquired via a 3D-turbo-field echo sequence that generated high-resolution T1-weighted images. Functional data were collected by using an asymmetric spin-echo, echo-planar sequence sensitive to BOLD contrast during 6-min functional runs. Following automated scout and shimming procedures, a high-resolution 3D MPRAGE sequence (TR = 6.787 ms, TE = 3.13 ms, flip angle = 8°, voxel size = 1.0 × 1.0 × 1.2 mm) was collected for the positioning of subsequent scans. fMRI images (i.e. blood oxygenation level-dependent signal or BOLD) were acquired using T2*-weighted sequences (TR = 2500 ms, TE = 28 ms, flip angle = 90°, voxel size = 3 × 3 mm, slice thickness = 3.0 mm, number of slices = 40). A fixation dot (a white dot centered on a black background) was displayed to subjects via a rear projection

system. Participants were instructed to stay awake, remain very still and stare at the fixation dot during functional runs.

Lesion Mapping and Percent Network/Node Destruction Calculations

Lesion mapping was done in a manner similar to Nomura et al. (2010). Lesion masks were drawn in FSLview by MCE (a board certified neurologist) in native space on the basis of the patient's T1-weighted anatomical scan by visually delineating the borders of encephalomalacia and white matter damage on axial, coronal, and sagittal slices. These lesion masks were then transferred into standard (MNI) space to allow for calculations of overlap with regions of interest (ROIs). Percent destruction of a given network was calculated as the number of cortical voxels in each patient's lesion mask which overlapped with the total number of voxels contained in the sum of all cortical network regions ascribed to the network. Percent destruction of a specific network node/ROI was calculated as the number of cortical voxels in each patient's lesion mask which overlapped with the total number of voxels in that specific node/ROI. This computation yielded a percentage damage for each patient for each network, and for each network node/ROI. Network ROIs (51 total, right, and left hemisphere) were directly taken from those detailed in a 7-network (default, limbic, ventral attention/salience, dorsal attention, frontoparietal control, somatomotor, and visual) parcellation in Yeo et al. (2011). Notably, this parcellation was derived by analyzing 1000 participants which were also part of the database from which we derived our 1139 participant sample. Figure 1 shows lesion masks for all 12 patient participants rendered in native space, as well as the percentage breakdown of each patient's lesion by network destroyed. Overall, while lesions affected both hemispheres, they were more likely to occur on the right (Table 1).

Functional diaschisis was assessed by studying functional couplings between undamaged ROIs. We were particularly interested in correlations among undamaged regions within the DN, as well as negative correlations between the DN and somatomotor and attentional (dorsal attention and ventral attention/salience) networks. Quantitatively, we considered a given ROI as being *undamaged* if it was <10% destroyed in *every one* of the patient participants, and *damaged* if *any* of the patients exhibited greater than this degree of injury. By these criteria, the visual and somatomotor networks were undamaged in all 12 patients. In the dorsal attention network, 1/6 ROIs-the left frontal eye field (lFEF)- was 21% damaged in Patient 1 (undamaged in all other patients), and was thus excluded from further analyses. The other five nodes were considered undamaged. In the ventral attention/salience network 6/11 ROIs were damaged (and excluded from further analysis), as they are situated in mid-cingulate and prefrontal cortices. Seven out of 16 ROIs in the frontoparietal control network were considered damaged, as they are also situated in prefrontal and cingulate cortices. Given

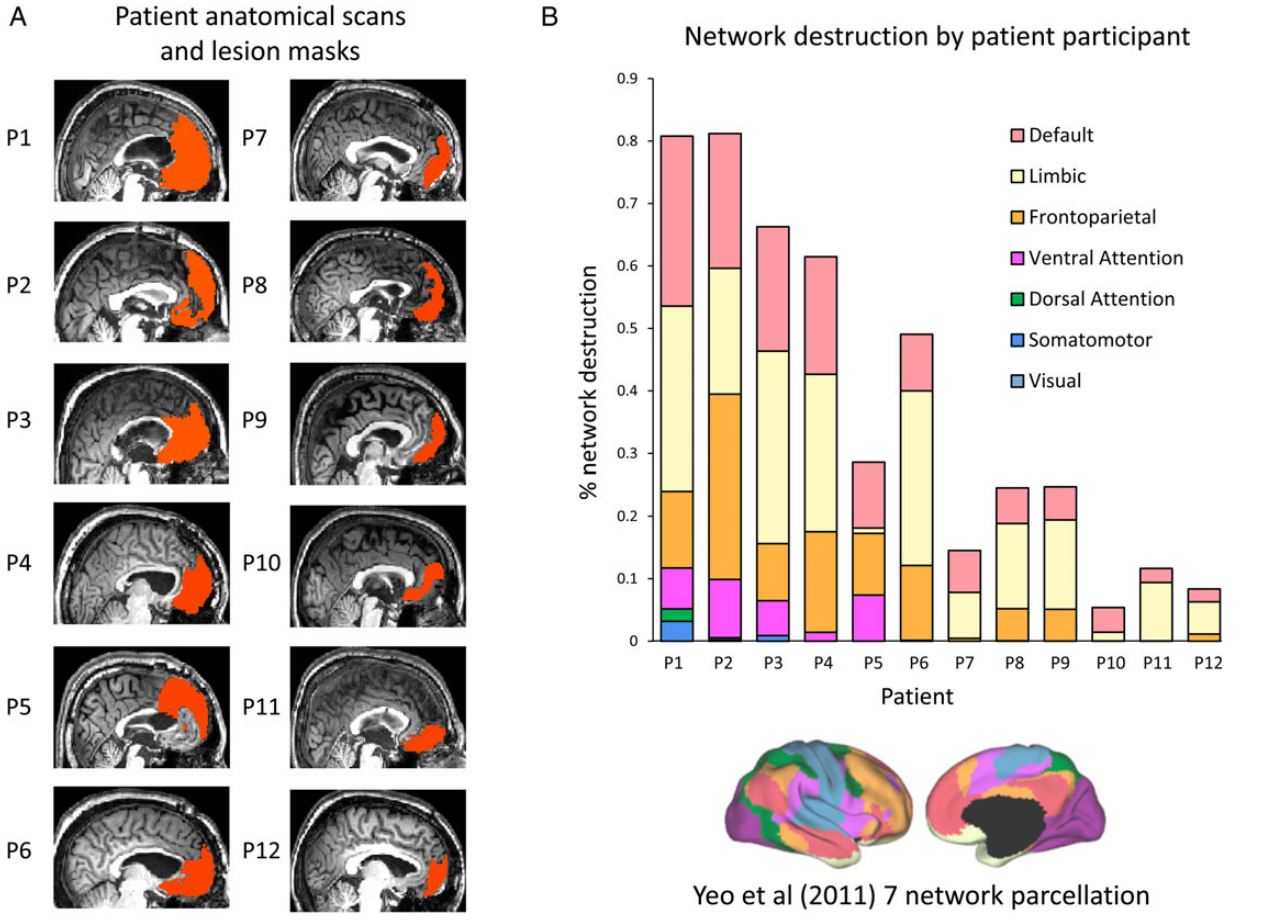

Figure 1. Individual patient network destruction: (*A*) representative T1 anatomical sagittal slices in native space for all 12 patient participants with overlay of lesions in red. (*B*) Percentage destruction of each of the seven networks described in Yeo et al. (2011) (shown in the bottom right) for each of the 12 patient participants. Patient participants are arranged from greatest to least default network (DN) damage.

our interest in negative correlations, and the fact that the fronto-parietal control network is not generally negatively correlated with the DN (Hutchison and Morton 2015), we primarily focused our analysis on undamaged nodes within the somatomotor and attentional networks.

fMRI Data Analysis

Functional MRI data were analyzed using a combination of freely available software packages (FSL, Freesurfer, SPM, 4dfp tools) and custom, in house software (Van Dijk et al. 2010). Preprocessing consisted of spatial normalization to a standard MNI 152 template brain, slice-timing correction, and motion correction. A second preprocessing stage removed nuisance variables (global mean, six motion parameters, and their derivatives, white matter and CSF), low-passed the data for signals >0.08 Hz (while retaining all frequencies below this), and smoothed the data spatio-temporally (6 mm FWHM Gaussian blur). After preprocessing, region-to-region correlation strengths, the main outcome measure of interest, were calculated with volumetric seed-based FC analyses: correlation maps were produced by extracting the BOLD time course from a "seed" region in the brain, and then computing the correlation coefficient between that time course and the time course from all other brain voxels. This method has been described in several other paradigms (Biswal et al. 1995; Fox et al. 2005; Vincent et al. 2008). Fifty-one seeds covering both hemispheres (26 left hemisphere and 25 right hemisphere), which were identical to those employed in the 7-network parcellation in Yeo et al. (2011), were utilized for all intrinsic FC analyses. These seeds were not spheres centered on specific coordinates, but rather were varying sizes and corresponded exactly to the parcels displayed in figure 11 in Yeo et al. (2011). Cerebellar seeds were not used as part of the analysis. Correlation strength between two seed regions was measured by the correlation coefficient, r, using Pearson's product–moment formula. We then employed Fisher's r-to-z conversion that transformed r values to corresponding values within the z distribution for all subsequent data analyses.

Quality Control Measures

Registration

Automated registration procedures were performed in SPM using procedures outlined in Van Dijk et al. (2010). Specifically, automated registration involved computing affine and nonlinear transforms connecting the first volume of the functional run using SPM2, with a T1 EPI template in MNI space. However, owing to concerns that this registration may be inaccurate because of the large size of the mPFC lesions, and possible difficulty delineating the demarcations of frontal landmarks due to frontal encephalomalacia, we visually examined each patient's automated registration to confirm that proper alignment to MNI space was achieved. Representative examples of registration for patients with large lesions (Patients 1 and 3) and their corresponding matched healthy comparisons are displayed in Supplementary Figure 1. We also examined the validity of transformations into MNI space of lesion masks drawn in native space for every patient. In order to achieve optimal registration of lesion masks, two patient lesion masks were re-aligned to MNI space in AFNI by manually delineating anatomical landmarks.

Head Motion

Because of significant concerns that head motion could alter inter-regional FC (Van Dijk et al. 2012), and because there was an anticipation that head motion might be higher in patients (Fox and Greicius 2010)—thus artificially accentuating differences in intrinsic FC between the patient and comparison groups—we took the following measures to address this confound. First, in instructing participants, particular emphasis was placed on remaining as still as possible to limit head movements. More significantly, a rigorous extended quality control analysis was performed on the functional data collected. This included slice signal-to-noise ratio (SNR), volume SNR, relative mean movement, relative-maximum movement, absolute-maximum movement, total number of movements over 1 mm, and total movements over 5 mm. As suspected, across all functional runs slice and volume-based SNR was lower for patients, and all other movement parameters were higher in patients; with volume SNR being statistically significant on a two sample unpaired t-test with equal variances assumed ($P = 0.01$); and with absolute maximum movement being almost significant ($P = 0.06$). As such, we only analyzed two functional runs for each participant. On the basis of a motion parameter measuring the maximum relative motion across an individual run, we took the two functional runs from patient participants with the least movement, and the two functional runs from the comparison participants with the most (worst) movement and carried these further for the main analyses. After doing so, all movement parameters tested were not statistically different between patients and their matched comparisons across the selected runs. Specifically, employing a two sample unpaired t-test with equal variances assumed, the patients and comparisons did not differ with respect to slice SNR ($t = 0.60$, mean difference = 21.3, $P = 0.56$), volume SNR ($t = -1.38$, mean difference = –6.5, $P = 0.18$), relative mean movement ($t = -0.20$, mean difference = –0.003, $P = 0.85$), relative-maximum movement ($t = -1.39$, mean difference = –0.20, $P = 0.18$), absolute-maximum movement ($t = 0.46$, mean difference = 5.8, $P = 0.65$), total number of movements over 1 mm ($t = -1.61$, mean difference = –1.1, $P = 0.12$), and total movements over 5 mm ($t = 0.68$, mean difference = 0.14, $P = 0.50$).

Global Signal

It is possible that large cortical lesions could alter the global signal in unknown ways and introduce artifactual intrinsic FC differences between patients and comparisons. This could conceivably occur through global or perilesional alterations in cerebral perfusion and/or neurovascular coupling. To approach this potential confound, we first compared mean global signals between the entire brain (lesion included) and the entire brain with lesioned cortex subtracted out in each of the 12 patient participants. Global signals were nearly identical between these two measurements, with r values being >0.99 in all patient participants (Supplementary Fig. 2A). The global signal of the lesion mask only differed from that of the whole brain when a smaller sample of the mask was sampled (Supplementary Fig. 2A). Next, we applied fast Fourier transformations to the global signals (Supplementary Fig. 2B), and found that amplitudes across ten frequency bins were not statistically different between the patient and comparison participants (all $P > 0.05$, P range = 0.17–0.94). Third, we found no statistically significant correlation between the amplitudes across the 10 frequency bins and the extent of lesion size in patient participants (all $P > 0.05$, P range = 0.11–0.86, r range = –0.06 to 0.48). Lastly, we examined cortical regions most highly correlated with the global signal in patients and comparisons, a method employed by Fox et al. (2009). Consistent with findings from that study, regions most highly correlated with the global signal in comparisons and patients included primary and secondary visual cortex, thalamus, and dorsal mid-cingulate (but not anterior cingulate) regions (Fox et al. 2009), and these patterns were qualitatively similar

between patients and comparisons. In contrast, mPFC was one of the least correlated regions in comparisons and patients, suggesting that mPFC lesions were unlikely to have profoundly affected the global signal (Supplementary Fig. 2C).

Graph Theoretical Analyses

The average comparison and patient 51-region cross-correlation matrices were transformed back into correlation values and binarized with an absolute threshold of $r > |0.5|$, with values greater than this threshold indicating a connection (edge) between the regions (nodes). We were specifically interested in assessing graph theoretical metrics that correlate with a given node's hub properties: that is node degree (the number of edges of a node that connect it to other nodes) and betweenness-centrality (the number of shortest path lengths that pass through that node) (Buckner et al. 2009). Degree and betweenness-centrality were calculated using the Brain Connectivity Toolbox (BCT; http://www.brain-connectivity-toolbox.net). In patients, regions of damage were included in the analysis.

Statistical Analysis

Our main outcome of interest was the difference in region-to-region z-scores within the DN and between the DN and attentional and somatomotor networks between patient and comparison groups. First, to ensure that our comparison group was reflective of the general population, we compared region-to-region z-scores between the comparison group and those derived from the large sample of 1139 healthy participants. These groups were compared with a Kolmogorov–Smirnov test, which assessed whether the probability distribution of z-scores of a given functional coupling in the comparison group could be derived from the corresponding z-score distribution in the larger ($n = 1139$) dataset. None of the DN functional couplings we examined were significantly different between the comparison and $n = 1139$ dataset at a P threshold 0.01. At a threshold of $P < 0.001$ (uncorrected), one DN functional coupling, right to left lateral temporal cortex (rLTC–lLTC), differed between the two groups. With respect to the negative correlations we examined, only one functional coupling, left posterior inferior parietal lobule (lpIPL) to right frontal eye field (rFEF), was significantly different between the two groups at a threshold of $P < 0.01$ (uncorrected).

Differences in region-to-region z-scores between comparison and patient groups were analyzed via two sample unpaired t-tests with equal variances assumed. Additional statistical tests included correlations between z-scores and lesion size in the patient group. Due to the relatively small sample size of the patient and comparison groups, and the difficulty in determining if the data met assumptions for parametric tests, we performed bootstrapping on every statistical that was significant (i.e. $P < 0.05$). Bootstrapping was performed with 25 000 samples in order to determine bias-corrected and accelerated confidence intervals (BCa) (Wichmann and Hill 2001).

For graph theoretical analyses, null models ($n = 25\,000$) were generated to test the node-wise significant differences between the patient and comparison populations through permutation testing. To compare degree, the binarized matrices were randomly reordered preserving the number of connections within the graph. To compare betweenness-centrality, the graphs were rewired while preserving node degree distribution. Significantly different (corrected for multiple comparisons using the Bonferroni correction) nodes were defined as those in which all the permuted differences between the node values of the two populations was less than that in the true data in fewer than 24 iterations ($P < 0.05/51$ regions $\times$ 25 000 iterations).

Results

Evidence that Lesions Included the DN's mPFC Node

We first sought to confirm that we were successful in selecting lesions that preferentially affected the mPFC portion of the DN. As displayed in Figure 2A, lesion distribution topographically

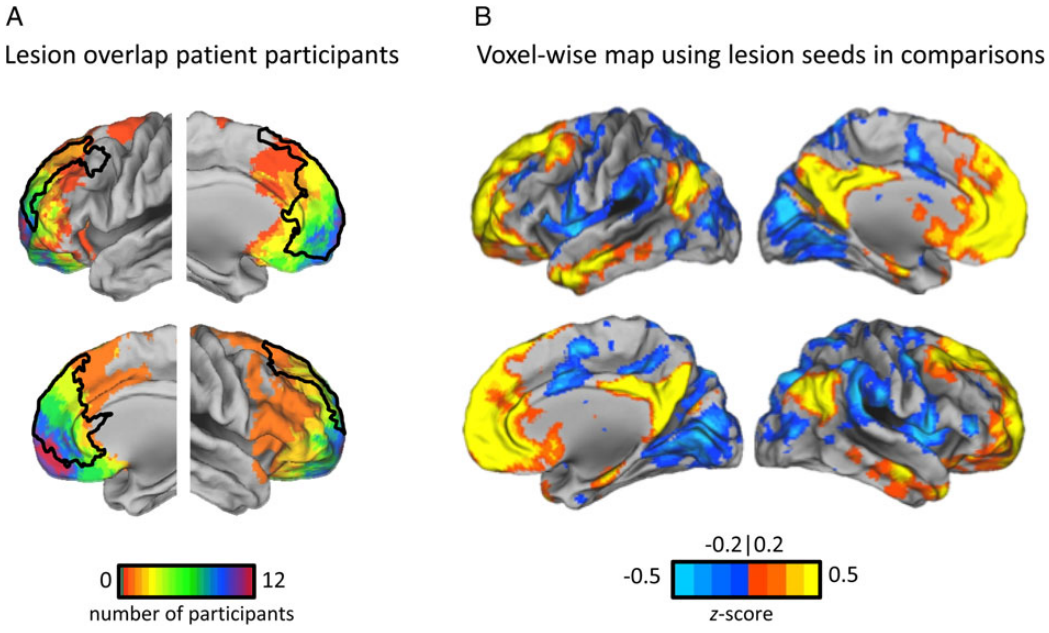

Figure 2. Validation that lesions affected the mPFC node of the DN: (A) lesion overlap across the 12 patient participants, as well as its anatomical overlap with the DN mPFC region in Yeo et al. (2011) (represented by a black outline). (B) Surface rendered mean seed-based FC voxel-wise maps created by seeding, in their matched healthy comparisons, the individual lesion masks of the 12 patients. The map shows strong intrinsic FC between the lesion seeds and canonical portions of the DN.

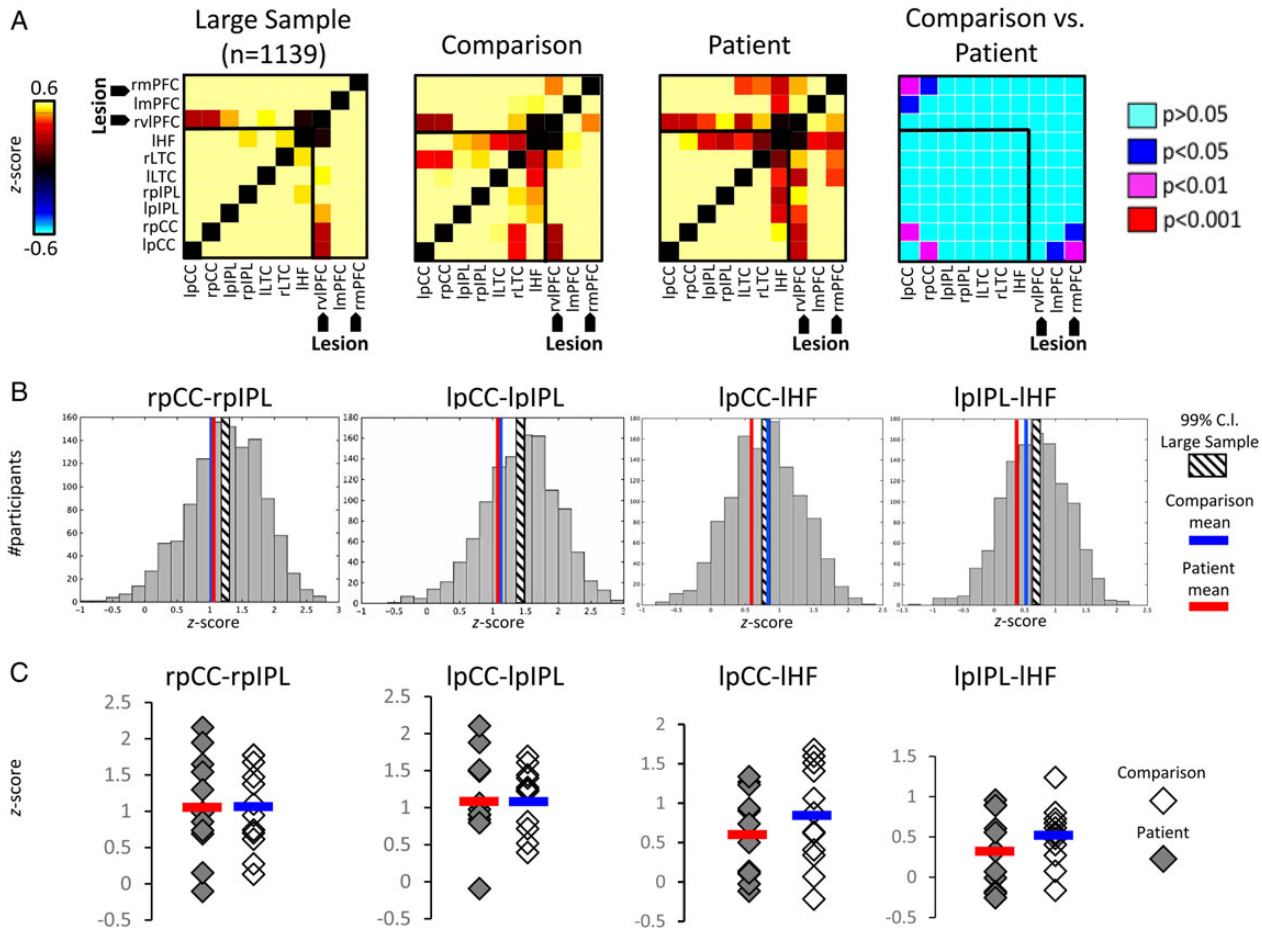

Figure 3. Preservation of DN intrinsic FC in patients: DN intrinsic functional connectivity (FC) comparisons across groups. All seeds are derived from the Yeo et al. (2011) parcellation. (*A*) Correlation matrix of intrinsic FC within the DN in the large sample of 1139 healthy participants, 12 comparison participants and 12 patients and the statistical differences between the patient and comparison groups. Correlations which involve undamaged cortex are outlined by black lines and black arrows (*B*) Histograms of the distribution of *z* scores for four representative DN coupling pairs. Superimposed on these are the 99% confidence interval of the distribution (hashed box) and the patient (red line) and comparison (blue line) means, which are comparable across groups (*C*) Plots of *z* scores for the same four coupling pairs showing overlap between patients and comparisons. The horizontal lines represent group means. l and r pCC, left and right posterior cingulate/ventral precuneus; l and r pIPL, left and right posterior inferior parietal lobule; l and r LTC, left and right lateral temporal cortex; lHF, left hippocampal formation; rvlPFC, right ventrolateral PFC; l and r mPFC, left and right medial prefrontal cortex.

overlapped with DN demarcations in prefrontal cortex obtained by Yeo et al. (2011). Overlap was maximally present in anterior and ventral regions of the mPFC portion of the DN, and in the right hemisphere maximum overlap extended into the limbic network as defined by Yeo et al. (2011). Figure 2*B* demonstrates that using lesion masks as seeds in individually matched healthy comparison participants yielded a connectivity pattern which strongly recapitulates the DN, with robust intrinsic FC emerging between the averaged lesion masks and established nodes of the DN: pCC, bilateral pIPL, bilateral hippocampal formation (HF) and bilateral LTC.

DN Changes

Next, we investigated DN intrinsic FC between patients and comparison participants. Comparisons were made among all 10 DN seeds represented in Yeo et al. (2011) and covering both hemispheres. As can be appreciated in Figure 3*A*,*B*, DN intrinsic FC was qualitatively and quantitatively very similar between the 1139 participant sample and our comparison sample. Expectedly, and consistent with Lu et al. (2011), given the significant destruction of mPFC and surrounding white matter tracts; patients, when contrasted with the comparison group, demonstrated a reduction in intrinsic FC between mPFC seeds and undamaged pCC (Table 2, Fig. 3*A*). However, despite our prediction that functional couplings would be disrupted throughout the remainder of the DN, patients demonstrated no statistically significant decreases in intrinsic FC among the majority of undamaged DN nodes when compared with comparison participants, and exhibited a connectivity profile similar to those of the 1139 sample (Table 2 and Fig. 3). Mean *z*-score values were similar across patient and comparison groups—both were similar to the 99% confidence interval of the distribution of *z*-scores in the 1139 sample (Fig. 3*B*). The only significant DN differences between patient and comparisons among undamaged DN nodes were between left and right divisions of pCC ($P = 8.7 \times 10^{-3}$, BCa = 0.24–0.83). Individual participant correlations shown in Figure 3*C* suggest that the lack of a statistical difference was not driven by outliers in the patient group, nor by larger variability in one group versus the other. Moreover, connectivity patterns among the patient, comparison and the 1139 sample were not substantially different on voxel-wise maps employing DN seeds (Fig. 4).

Importantly, this preservation of DN intrinsic FC was also seen at the individual patient level; including in Patient 1, who suffered overwhelming and encompassing mPFC damage (Fig. 4A). Lending further support to the fact that mPFC damage did not appreciably affect undamaged DN functional couplings, the percent of DN destruction across patient participants did not correlate with the strength of intrinsic FC between nonlesioned DN nodes (Fig. 7A, Table 4).

Table 2 Default network functional couplings among lesioned and undamaged cortex in patients versus comparison

Functional coupling	Significance level patient versus comparison
DN functional couplings involving lesioned mPFC	
lpCC–rmPFC	$P = 3.2 \times 10^{-3}$, BCa = 0.37–1.34
lpCC–lmPFC	$P = 0.03$, BCa = 0.04–0.89
rpCC–rmPFC	$P = 0.03$, BCa = 0.10–1.07
DN functional couplings among undamaged nodes	
rpCC–rpIPL	$P = 0.98$
lpCC–lpIPL	$P = 0.91$
rpIPL–lpIPL	$P = 0.15$
lpCC–lHF	$P = 0.33$
lpIPL–lHF	$P = 0.33$
rLTC–lLTC	$P = 0.74$

The top panel shows functional couplings involving lesioned cortex that were significantly weakened in patients. The bottom panel shows major functional couplings among undamaged DN nodes which were not different between patient and comparison groups.
BCa, bias-corrected and accelerated confidence intervals derived from Bootstrapping with 25 000 samples.

Effects in Other Networks

No statistically significant intrinsic FC changes were detected between the patient and comparison groups among undamaged homologous regions of the visual (right to left visual seeds) or somatomotor (right to left somatomotor seeds) networks. The frontoparietal control network demonstrated significant changes between undamaged regions among only three coupling pairs, and all three involved a small precuneus seed abutting (and arguably a portion of) pCC. The dorsal attention network had one significant difference among undamaged regions in a small node approximating the lesions in precentral ventral cortex (PrCv) (left to right PrCv: $P = 0.02$, BCa = 0.22–1.08). In contrast, the ventral attention/salience network displayed more significant intranetwork intrinsic FC changes among undamaged regions. These included functional couplings with two undamaged frontal regions: fronto-opercular/fronto-insular cortex (FrOper) and precentral cortex (PrC). Specifically, the following functional couplings were significantly different: lFrOper and right Supramarginal cortex (rSupMar) ($P = 0.02$, BCa = 0.11–1.08), rSupMar and left SupMar ($P = 0.04$, BCa = 0.10–1.31), rPrC and left Temporo-occipital cortex ($P = 0.01$, BCa = 0.05–0.77), rPrC and left SupMar ($P = 4.0 \times 10^{-3}$, BCa = 0.25–1.61), and rPrC and left FrOper ($P = 0.03$, BCa = 0.25–1.61).

Internetwork Effects

We next examined whether mPFC damage would affect functional relationships between the DN and undamaged regions of other large-scale cortical networks to which it is negatively correlated. Negative correlations between pCC and multiple nodes of attentional and somatomotor networks were significantly weaker

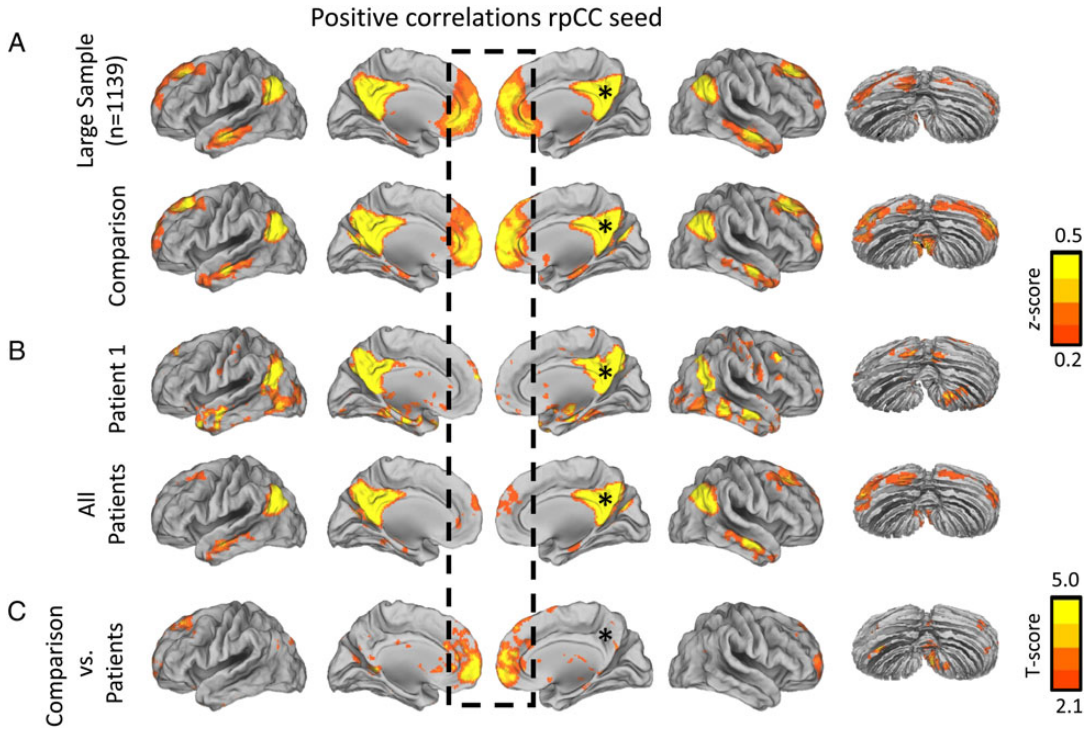

Figure 4. Preservation of DN instrinsic functional connectivity in patients: Surface rendered mean voxel-wise intrinsic FC maps (including the cerebellum, right) derived from a rpCC seed (represented by asterisks) across groups. The dashed box highlights mPFC. Only positive correlations are shown. (*A*) Maps derived from a rpCC in the large sample of 1139 healthy subjects and in the 12 comparison participants. (*B*) Maps derived in the patient with the greatest mPFC damage and across all 12 patients showing an absence of FC with mPFC, but preservation of DN FC among undamaged DN nodes. (*C*) Voxel-wise T map showing statistically significant differences between comparison and patient groups, which are only apparent between rpCC and mPFC.

Table 3 Negative functional couplings significantly different patients and comparisons

	Significance level patient versus comparison
Functional coupling (pCC to other networks)	
rpCC–lSomMot	$P = 1.2 \times 10^{-3}$, BCa = −1.41 to −0.43
lpCC–lSomMot	$P = 5.1 \times 10^{-3}$, BCa = −0.98 to −0.26
rpCC–rSomMot	$P = 4.3 \times 10^{-3}$, BCa = −1.10 to −0.34
lpCC–rSomMot	P = 0.02, BCa = −0.95 to −0.19
rpCC–lSPL/MT+	P = 0.03, BCa = −1.06 to −0.12
lpCC–lSPL/MT+	P = 0.04, BCa = −0.92 to −0.04
rpCC–rSPL/MT+	P = 0.03, BCa = −0.97 to −0.11
rpCC–lPrCv	P = 0.03, BCa = −0.99 to −0.08
lpCC–lPrCv	P = 0.03, BCa = −0.92 to −0.07
rpCC–rPrCv	$P = 1.5 \times 10^{-4}$, BCa = −0.95 to −0.36
lpCC–rPrCv	$P = 5.1 \times 10^{-4}$, BCa = −0.81 to −0.26
rpCC–rFEF	P = 0.04, BCa = −1.09 to −0.04
rpCC–lSupMar	P = 0.02, BCa = −0.92 to −0.19
lpCC–lSupMar	P = 0.02, BCa = −0.83 to −0.09
rpCC–rSupMar	P = 0.03, BCa = −0.83 to −0.07
rpCC–lFrOper	P = 0.01, BCa = −0.75 to −0.21
lpCC–lFrOper	P = 0.02, BCa = −0.72 to −0.09
rpCC–rPrC	$P = 4.1 \times 10^{-3}$, BCa = −0.98 to −0.27
lpCC–rPrC	$P = 3.5 \times 10^{-3}$, BCa = −0.86 to −0.23
Functional couplings (rpIPL to other networks)	
rpIPL–rSomMot	$P = 9.1 \times 10^{-3}$, BCa = −0.79 to −0.24
rpIPL–lSomMot	P = 0.01, BCa = −0.68 to −0.27
rpIPL–rPrCv	P = 0.02, BCa = −0.81 to −0.11
rpIPL–rSupMar	P = 0.01, BCa = −0.74 to −0.17
rpIPL–rPrC	P = 0.01, BCa = −0.80 to −0.22

(i.e. less negative, and occasionally even positive) in the patient versus the comparison and 1139 participant groups (Table 3, Figs 5 and 6). Notably, this qualitatively extended to negative correlations between pCC and cerebellar regions, as can be appreciated in the voxel-wise maps displayed in Figure 6. In addition to pCC, right (but not left) pIPL exhibited negative correlation differences between patients and comparisons (Table 3). Critically, across all 12 patients the extent of DN damage correlated with the extent to which negative correlations were decreased between pCC and attentional and somatomotor networks, with 7/11 negative correlations being statistically significant (Fig. 7*B*, Table 4).

There were no significant differences in functional couplings between the DN and the frontoparietal control network between the patient and comparison groups. However, these correlations were not reliably negative in the comparison group, nor in the $n = 1139$ dataset. Notably, although frontoparietal control network damage was significant in some patients, this did not correlate as well with decreases in negative correlation strength. Of the 11 correlations examined in Figure 7*B*, only two: lpCC–lSomMot ($r = 0.65$, $P = 0.02$, BCa = 0.26–0.88) and lpCC–lSupMar ($r = 0.63$, $P = 0.03$, BCa = 0.19–0.91) significantly correlated with the extent of frontoparietal control network damage.

A possible explanation for the decreased negative correlations between pCC and perilesional regions (e.g. FrOper, PrCv, PrC) is that these regions were uniquely affected by neurovascular changes accompanying the lesion due to their proximity to it. However, we found equally significant alterations in negative functional couplings between pCC and posterior cortical regions anatomically distant from the lesion (Figs 5 and 6 and Supplementary Fig. 4).

Graph Theoretical Analyses

Graph theoretical analyses revealed that compared with healthy comparisons, patient participants demonstrated a weakening of hub properties in bilateral pCC ROIs. Consistent with several studies supporting that pCC has global hub properties, we found that right and left pCC exhibited among the highest degree and betweenness-centrality in the comparison participants (average degree = 22, average betweenness-centrality = 273). Figure 8 shows that mPFC exhibited high degree and betweenness-centrality in the comparison group as well, consistent with this region's global hub properties. Hub metrics were markedly lower in pCC in the patient group (average degree = 10.5, average betweenness-centrality = 47), and statistically significantly different from comparisons with respect to betweenness-centrality. While it would be expected that a general decrease in count-based measures would arise from lesions of nodes within a graph, we observed a nonuniform pattern of decreases in degree and betweenness-centrality in patients. That is, betweenness-centrality was specifically decreased in bilateral pCC, and not in other cortical regions, suggesting a change not solely attributable to a decrease in node number. In fact, given pCC's central role and high degree, the degree and betweenness values were expected to actually be less susceptible to node deletion than less connected regions. Moreover, we also observed nonuniform *increases* in hub metrics in patients in orbital and dorsolateral prefrontal cortex, rpIPL and rLTC.

Discussion

This study is among the first to investigate the intrinsic FC effects of damage to a putative hub of a large-scale network comprised of multiple interacting association cortices. Somewhat surprisingly, we found that mPFC damage was more likely to alter intrinsic functional couplings between the DN and other networks then it was to affect functional relationships within the DN proper. This result is inconsistent with prior depictions of mPFC as a key DN hub, insofar as the network remained functionally viable in the setting of large mPFC lesions. Rather, our observations resonate with other studies that have emphasized distributed, extranetwork effects of hub lesions (Gratton et al. 2012). More specifically, our results invoke a model wherein certain nodes of functionally heterogeneous networks may be tasked with facilitating communication between their native network and other large-scale systems. In turn, this would raise the possibility that certain lesion-induced clinical deficits arise because of breaches in internetwork information exchange.

Lack of Observed Intranetwork Effects

The lack of observed DN intrinsic FC changes can be reconciled by evidence that mPFC is both structurally and functionally dissociable from the remainder of the network. Anatomically, macaque area 23 (posterior cingulate cortex) has robust connections with area 7a (the putative homolog of human pIPL) and with the medial temporal lobe (Barbas et al. 1999; Kobayashi and Amaral 2007; Buckner et al. 2008). In contrast, areas 23 and 31 (pCC) and area 30 (retrosplenial cortex) send weaker projections to mPFC (pCC and retrosplenial projections are more strongly directed toward lateral PFC) (Kobayashi and Amaral 2007). Furthermore, in humans, maturation of mPFC–pCC structural connectivity (which is mediated by longer distance connections in the cingulum bundle) is delayed compared with other DN structural connections (Supekar et al. 2010). Functionally, on the basis of task-evoked activity, the DN has been divided into subsystems

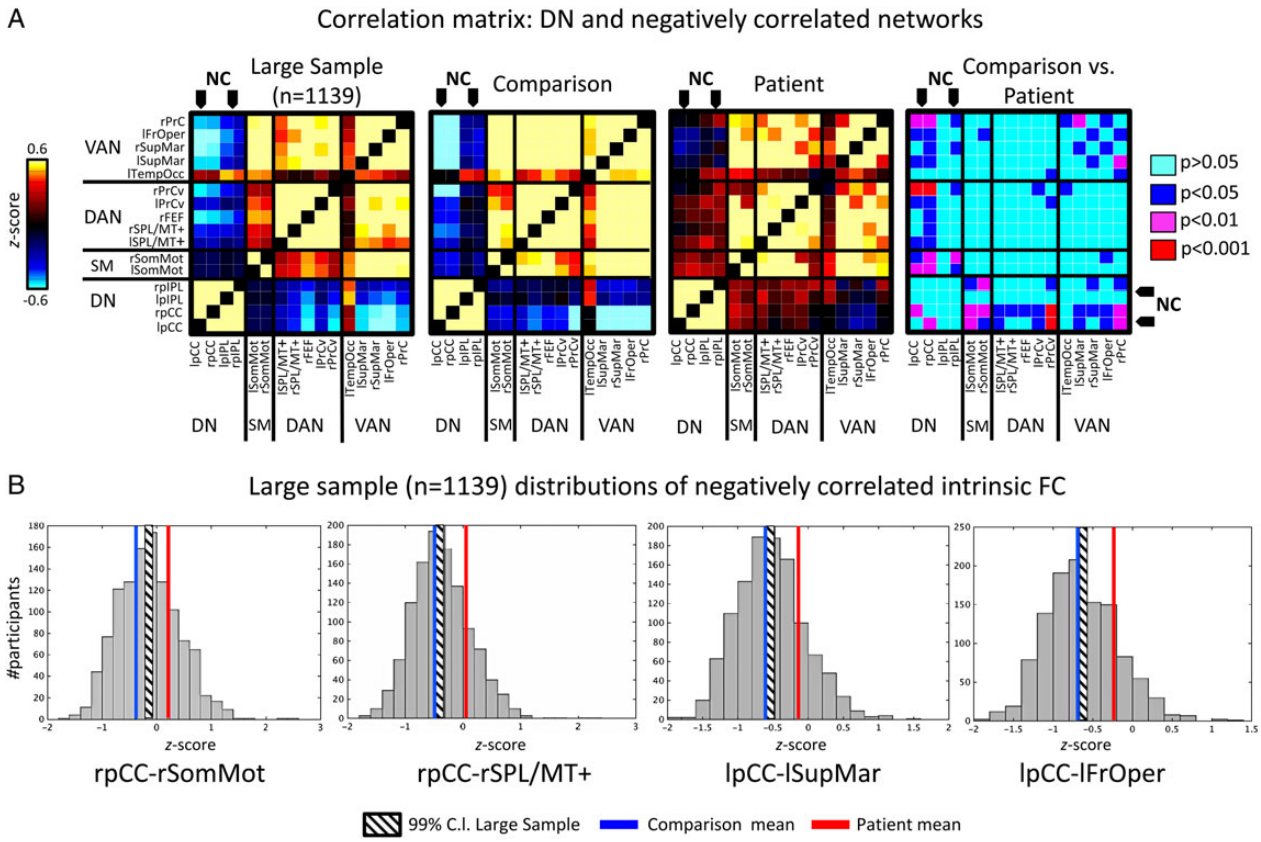

Figure 5. Weaker negative correlations in the patient group: (*A*) Correlation matrix across the three groups of connectivity between the DN (bilateral pCC and bilateral pIPL seeds) and *undamaged* seeds of somatomotor (SM), dorsal attention (DAN), and ventral attention/salience (VAN) networks. Decreased negative correlations are seen in patients, particularly with bilateral pCC. Negative correlations (NC) are highlighted with black arrows. (*B*) Histograms of the distribution of z scores for four representative negatively correlated coupling pairs. Superimposed on these are the 99% confidence interval (hashed box) and the patient (red line) and comparison (blue line) means. Patient mean differs from the comparison mean and large sample distribution. l and r SomMot, left and right somatomotor cortex; rFEF, right frontal eye fields; l and r SPL/MT+, left and right superior parietal lobule/MT+; l and r PrCv, left and right precentral ventral cortex; lFrOper, left fronto-opercular/fronto-insular cortex; l and r SupMar, left and right supramarginal cortex; rPrC, right precentral cortex; lTempOcc, left temporoccipital cortex.

responsible for mental perspective taking and self-referential thought on the one hand (mediated by mPFC), and episodic memory processing on the other (mediated by a parietal-hippocampal sub-network) (Fransson and Marrelec 2008; Uddin et al. 2009). mPFC also exhibits divergent thalamic intrinsic FC patterns (Yuan et al. 2016) and negative intrinsic FC patterns (Uddin et al. 2009) when compared with posterior portions of the DN. mPFC becomes functionally decoupled from the remainder of the DN during deep sleep (Horovitz et al. 2009). Lastly, mPFC lesions are likely to induce specific clinical deficits in affective processing (see below) which are not observed with lesions involving posterior DN nodes.

An alternative explanation for the lack of DN FC changes is that networks composed of multimodal association cortices are better able to withstand isolated injury. Many of the prior lesion studies emphasizing intranetwork intrinsic FC changes have surveyed damage to sensorimotor circuits (Carter et al. 2010, 2012; van Meer et al. 2010; Wang et al. 2010; Rehme and Grefkes 2013). Sensorimotor regions are more likely to display short-range, modular connectivity (Sepulcre et al. 2010) and serial, hierarchical organizational profiles (Buckner and Krienen 2013). In contrast, heteromodal association cortex is more likely to exhibit long-range, diverse, and parallel connectivity patterns, with individual association regions themselves being inherently functionally heterogeneous (Yeo et al. 2015). Therefore, it is possible that association cortices are less functionally interdependent with one another, even when sharing a common network membership. The only other study (to our knowledge) to assess intrinsic FC aberrations in the setting of DN lesions examined patients with hippocampal sclerosis (Frings et al. 2009). Of note, although these authors found intra-DN FC changes in the patient group, these changes were limited to couplings between the precuneus and the lesion itself (left hippocampus) and to couplings between the precuneus and ipsilesional temporal cortex.

mPFC Lesions Alter the Functional Homeostasis Between Cortical Networks

In our study mPFC lesions did induce network-specific effects, insofar as negative correlations between the DN and attentional and somatomotor networks were weakened in patients. Some authors have argued that negative correlations are the artifactual consequence of global signal regression during preprocessing (Murphy et al. 2009), and therefore not reflective of neurobiologically based relationships between brain networks. However, this position is contradicted by several studies supporting a physiological basis for negative correlations, as well as supporting their existence in the absence of the use of global signal regression (Fox et al. 2009; Scholvinck et al. 2010; Smith et al. 2012; Keller et al. 2013; Yang et al. 2014; Hutchison et al. 2015). Moreover, the contention that global signal regression artificially

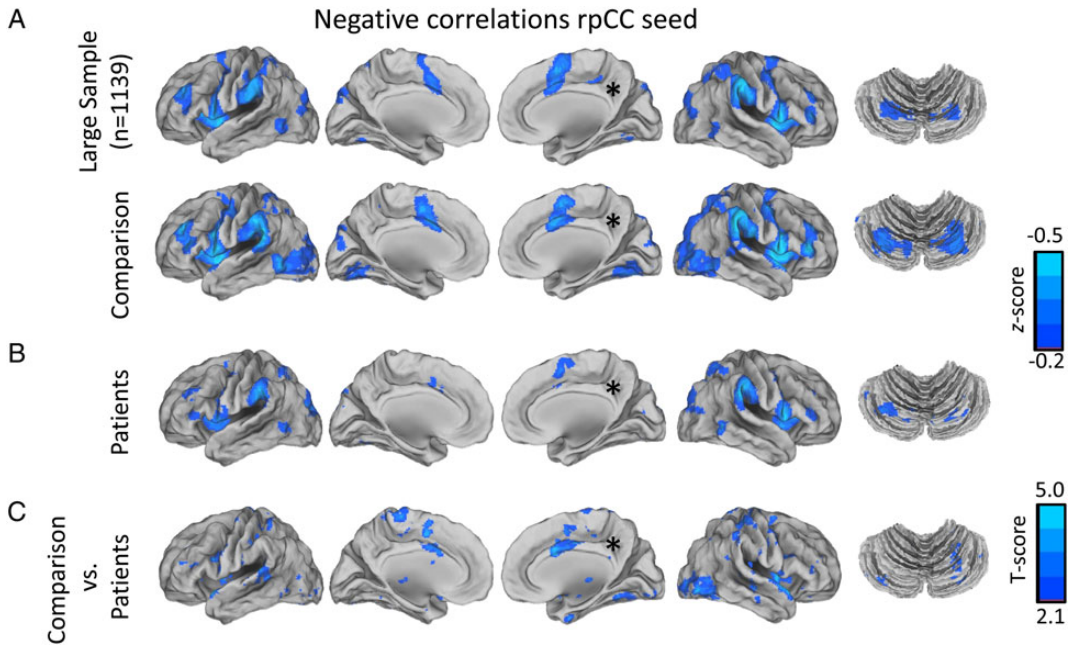

Figure 6. Weaker negative correlations in the patient group: surface rendered mean voxel-wise intrinsic FC maps (including the cerebellum, *right*) derived from a rpCC seed (represented by asterisks) across groups. Only negative correlations are shown. (*A*) Maps derived from a rpCC in the large sample of 1139 healthy subjects and in the 12 comparison participants. (*B*) Maps derived in the patient group. (*C*) Voxel-wise T map showing statistically significant differences between comparison and patient groups.

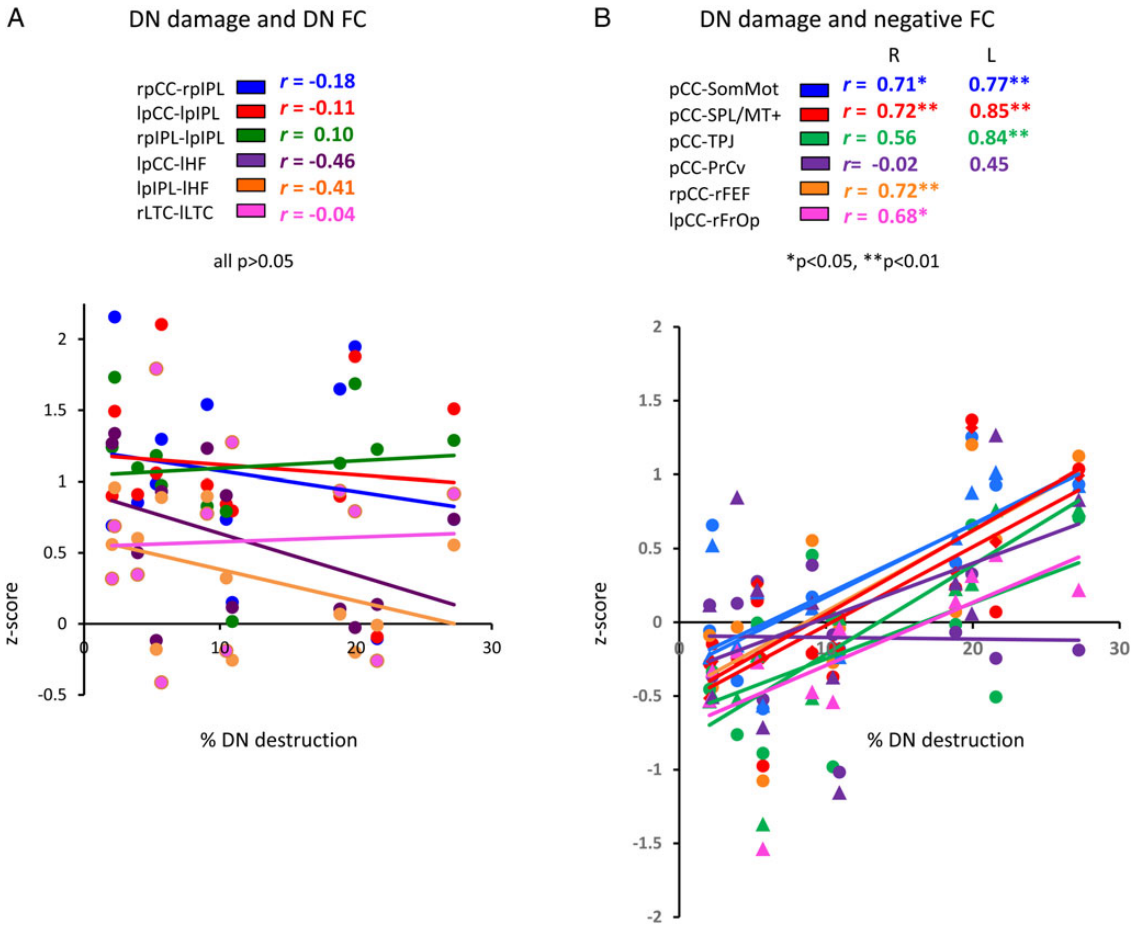

Figure 7. Correlation between z transformed correlations and percent of DN damage. (*A*) No significant association between region-to-region correlation coefficients within the default network (DN) and the extent of DN damage. (*B*) However, extent of (DN) damage *did* correlate with the degree of weakening of negative correlations between pCC and undamaged regions of negatively correlated networks. rpCC–rPrC not shown, which was nonsignificant.

Table 4 Correlations between degree of DN damage and z values in patients

	Correlation between DN damage and z-score across patients
Functional coupling (within the DN)	
rpCC–rpIPL	$r = -0.18$, $P = 0.58$
lpCC–lpIPL	$r = -0.11$, $P = 0.75$
rpIPL–lpIPL	$r = 0.10$, $P = 0.76$
lpCC–lHF	$r = -0.46$, $P = 0.14$
lpIPL–lHF	$r = -0.41$, $P = 0.18$
rLTC–lLTC	$r = -0.04$, $P = 0.89$
Functional coupling (pCC to other networks)	
rpCC–rSomMot	$r = 0.71$, $P = 0.01$, BCa = 0.21–0.93
lpCC–lSomMot	$r = 0.77$, $P = 4.0 \times 10^{-3}$, BCa = 0.42–0.94
rpCC–rSPL/MT+	$r = 0.72$, $P = 8.0 \times 10^{-3}$, BCa = 0.32–0.90
lpCC–lSPL/MT+	$r = 0.85$, $P = 1.0 \times 10^{-3}$, BCa = 0.43–0.99
lpCC–lSupMar	$r = 0.84$, $P = 1.0 \times 10^{-3}$, BCa = 0.46–0.99
rpCC–rFEF	$r = 0.72$, $P = 9.0 \times 10^{-3}$, BCa = 0.24–0.90
lpCC–lFrOper	$r = 0.68$, $P = 0.02$, BCa = 0.28–0.95
rpCC–rSupMar	$r = 0.56$, $P = 0.06$
rpCC–rPrCv	$r = -0.02$, $P = 0.94$
lpCC–lPrCv	$r = 0.14$, $P = 0.45$
rpCC–rPrC	$r = -0.07$, $P = 0.82$

Representative functional couplings within the DN did not correlate with percentage of DN destruction (0/6 significant), (*top*) while couplings between pCC and attentional and somatomotor networks did (7/11 significant) (*bottom*).

gave rise to our findings is argued against by a lack of differences in the global signal between patients and comparison participants (Supplementary Fig. 2).

A possible explanation for the aberrant negative correlations we observed is that the cortical midline (i.e. mPFC and pCC) plays a pivotal role in mediating internetwork communication. This hypothesis is consistent with evidence that the cortical midline is an integrator of global information transfer, with cortical midline lesions inducing the most widespread connectivity aberrations (Alstott et al. 2009). It is also possible that the internetwork effects of mPFC lesions were indirectly mediated through effects upon pCC. pCC has repeatedly been designated as a global cortical hub (by degree and centrality criteria) which exerts functional influence over varied cortical systems (Tomasi and Volkow 2011; Bullmore and Sporns 2012; Leech et al. 2012). Consistent with this, measures of degree and betweenness-centrality were highest in pCC in the comparison group, and betweenness-centrality was markedly weakened in pCC in patients. As such, it is possible that mPFC lesions weakened hub properties of pCC, and that this resulted in it having weaker functional relationships with attentional systems to which it is negatively correlated. Evidence that mPFC could causally effect pCC's functional status comes in directed effective connectivity studies showing a preferential directionality of information flow from mPFC to pCC, as opposed to vice versa (Miao et al. 2011; Di and Biswal 2014; Wu et al. 2014).

Alternatively, the weakened intrinsic FC within the ventral attention/salience network we observed (Fig. 5 and Supplementary Fig. 3) may have played a role in the weakened cross-network couplings. Prior reports have demonstrated a role for the ventral attention/salience network in mediating switching between executive and DN function (Sridharan et al. 2008), and for ventral attention/salience network damage affecting DN deactivations (Jilka et al. 2014). It is therefore possible that the patient lesions severed white matter connectivity between the DN and the ventral attention/salience network, and that this contributed to the abnormal cross-network connectivity.

Potential Behavioral and Clinical Implications of Altered Negative Correlations

There is an extensive literature from functional activation and lesion studies detailing the putative functional roles of mPFC. A common theme is that mPFC is involved in processing affectively relevant information. Ventral mPFC (vmPFC) appears to be heavily implicated in processing the value of stimuli, and is activated by several tasks involving value appraisal including: reward extinction, reversal learning, risk aversion, temporal discounting and regret (for review, see Fellows 2007). Furthermore, both vmPFC and more dorsal mPFC are significantly activated during self-referential ideation and mentalizing (Mitchell et al. 2005; Amodio and Frith 2006). Lesions to vmPFC/medial orbitofrontal cortex have been associated with impairments in reversal learning, response extinction, award reappraisal and financial decision-making (Bechara et al. 1997; Happaney et al. 2004). In addition, patients with vmPFC/medial orbitofrontal lesions can display disinhibition, impulsivity and aggression (Stuss 2011), while lesions encompassing anterior and mid-cingulate cortex can produce abulia or akinetic mutism (Devinsky et al. 1995; Stuss 2011). In this study, selected patients exhibited marked abulia (Patients 1, 3, and 6), disinhibition (Patient 2), and frontal-executive impairments (e.g. processing speed and working memory; Patients 1, 3, 5, and 9, Supplementary Table 2).

To date, such clinical deficits have largely been explained on the basis of impairments in *local* processing within portions of mPFC, or on the basis of abnormal processing between mPFC and limbic or autonomic centers. The clinical and behavioral sequelae of the negative correlations we observed cannot be addressed with the methodology we employed. Nevertheless, it is conceivable that certain clinical deficits observed in mPFC lesioned patients are rooted in altered relationships between large-scale networks. Generally, there is mounting evidence that negative correlations may reflect functional relationships important to flexible and efficient cognitive processing (Kelly et al. 2008). Moreover, a recent study demonstrated that negative intrinsic correlations underlie lesion-induced symptomatology across varied neuropsychiatric syndromes (Boes et al. 2015). More specifically, disinhibition can be the result of impaired top-down control exerted by regions functionally aligned with attentional networks (Dalley et al. 2011). Also, addictive disorders (which are characterized by aberrant reward processing) have been linked to weakened coupling between the DN and the negatively correlated ventral attention/salience network (Liang et al. 2015; Muller-Oehring et al. 2015). With respect to frontal-executive function, negative correlations become stronger during human development and weaken with advanced age, paralleling developmental improvements and declines in executive capabilities (Chai et al. 2014; Ferreira et al. 2015). In addition, the strength of negative correlations between medial and lateral prefrontal cortex correlates to working memory performance (Hampson et al. 2010), and has been associated with the mental inflexibility seen in schizophrenia (Whitfield-Gabrieli et al. 2009) and Attention Deficit Hyperactivity Disorder (Mattfeld et al. 2014). Taken together, our study raises the possibility of using longitudinal improvements in negative correlations as markers of clinical recovery in brain-injured patients, the feasibility of which has been shown with positive correlations (He et al. 2007; van Meer et al. 2010).

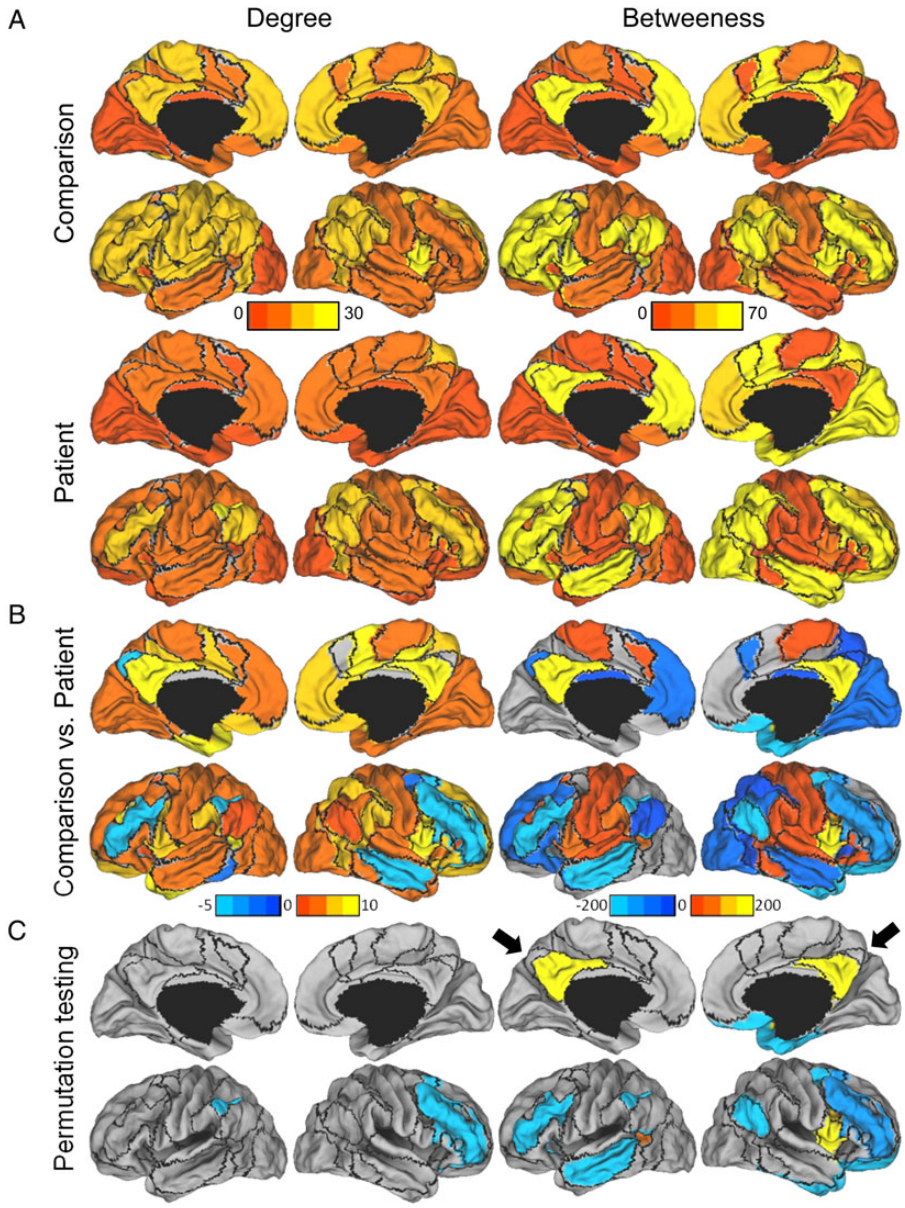

Figure 8. Decreased hub-like properties of pCC in the patient group: surface rendered maps of degree (*left panel*) and betweenness-centrality (*right panel*). Increases are represented in red-yellow and decreases in blue-light blue. Damaged regions were included in the analysis. (*A*) Maps for comparison (*top row*) and patient (*second row*) participants. (*B*) Differences between the two groups. (*C*) Statistical significant differences derived from permutation testing (Bonferroni corrected for multiple comparisons). Bilateral pCC demonstrates statistically significant decreases in betweenness-centrality in patients (black arrows).

Limitations

This study is limited by its cross-sectional nature, which prohibits knowledge of how the observed FC changes may have evolved over time. Longitudinal intrinsic FC studies of lesions in humans and animals have demonstrated that connectivity aberrations can normalize over the weeks to months following lesion acquisition (van Meer et al. 2010; Ovadia-Caro et al. 2013). However, the relatively large size of some of the mPFC lesions suggests that it was unlikely that a complete functional reorganization occurred (Murphy and Corbett 2009). Also, other studies of chronic lesions in humans have shown persistent, network-specific aberrations (Nomura et al. 2010). Moreover, in our study only selected functional couplings were preserved, while others remained abnormal. A potentially significant confound is the use of centrally acting medications in some patient participants, common to many human lesion studies. However, our participants were not taking medications that are known to significantly alter intrinsic FC, for example by markedly depressing alertness and/or consciousness (for instance see Heine et al. 2012; Liang et al. 2012). Second, similar findings were observed in patients who were not on any psychoactive medications. Third, fMRI task activation studies have demonstrated normalization (and not destabilization) of BOLD activation patterns in epilepsy patients treated with the anticonvulsant levetiracetam (Wandschneider et al. 2014; Beltramini et al. 2015). It is also unlikely that medications would affect certain functional couplings and not others. For example, the magnitudes of several positive and negative correlations did not differ between patients and comparisons. Finally, many of the patient lesions

included significant damage to medial orbitofrontal cortex, which is part of the limbic and not the default, network in the 7-network parcellation (Yeo et al. 2011). However, several parcellation schemes include the medial orbitofrontal cortex as being part of the DN, and this region's intrinsic FC profile significantly overlaps with that of other DN nodes (Yeo et al. 2013). Furthermore, other authors have noted that the dissociation of the DN into a distinct limbic network may be partially rooted in susceptibility artifacts and poor SNR in orbitofrontal cortex and anterior temporal cortex (Yeo et al. 2011; Power et al. 2013).

Conclusion

We observed that circumscribed DN lesions did not compromise the network's overall functional integrity. We posit that this is reflective of 1) mPFC's structural and functional independence from the remainder of the DN and 2) the general lack of interdependence between association cortices, even when they belong to the same network. The latter supposition would suggest that networks composed of multiple association cortices are unlikely to be functionally homogenous and functionally distinct systems whose component nodes synchronously cooperate toward common and specific behavioral goals (e.g. "internal mentation" in the case of the DN) (Leech et al. 2012). Instead, network membership among DN nodes may be just as rooted in shared interactions with cortical regions of other networks. If true, this would mandate that future studies examining the behavioral and clinical significance of the brain's intrinsic functional architecture explore dynamic interactions between cortical networks.

Authors' Contributions

M.C.E. designed and performed the research and wrote the paper. S.M., M.C.E., and R.M.H. analyzed the data. S.M., R.M.H., M.A.H., and A.P.L. helped interpret findings and contributed to the writing of the paper.

Supplementary Material

Supplementary material can be found at: http://www.cercor.oxfordjournals.org/.

Funding

Work on this study was supported in part by the Berenson-Allen Foundation, the Sidney R. Baer Jr. Foundation, grants from the National Institutes of Health (R01HD069776, R01NS073601, R21 MH099196, R21 NS082870, R21 NS085491, and R21 HD07616), and Harvard Catalyst|The Harvard Clinical and Translational Science Center (National Institutes of Health: National Center for Research Resources and the National Center for Advancing Translational Sciences, UL1 RR025758). M.C.E. was supported by the National Institute of Mental Health Mentored Patient-Oriented Research Career Development Award (K23MH099413), and by a Brain and Behavior Young Investigator Award. R.M.H. was supported by a Canadian Institutes of Health Research postdoctoral fellowship.

Notes

We thank Andrew Ellison and the Center for Biomedical Imaging at Boston University for assistance in collecting the rs-fMRI data and Michael P. Alexander, MD for assistance with patient recruitment. Data for the 1139 subject comparisons were provided [in part] by the Brain Genomics Superstruct Project of Harvard University and the Massachusetts General Hospital (Principal Investigators: Randy Buckner, Joshua Roffman, and Jordan Smoller), with support from the Center for Brain Science Neuroinformatics Research Group, the Athinoula A. Martinos Center for Biomedical Imaging, and the Center for Human Genetic Research. Twenty individual investigators at Harvard and MGH generously contributed data to the overall project. The content is solely the responsibility of the authors and does not necessarily represent the official views of Harvard Catalyst, Harvard University and its affiliated academic healthcare centers, the National Institutes of Health, or the Sidney R. Baer Jr. Foundation. *Conflict of Interest*: A.P.L. serves on the scientific advisory boards for Nexstim, Neuronix, Starlab Neuroscience, Neuroelectrics, Axilum Robotics, Magstim, Inc., and Neosync; and is listed as an inventor on several issued and pending patents on the real-time integration of transcranial magnetic stimulation (TMS) with electroencephalography (EEG) and magnetic resonance imaging (MRI).

References

Alstott J, Breakspear M, Hagmann P, Cammoun L, Sporns O. 2009. Modeling the impact of lesions in the human brain. PLoS Comput Biol. 5:e1000408.

Amodio DM, Frith CD. 2006. Meeting of minds: the medial frontal cortex and social cognition. Nat Rev Neurosci. 7:268–277.

Andrews-Hanna JR, Reidler JS, Sepulcre J, Poulin R, Buckner RL. 2010. Functional-anatomic fractionation of the brain's default network. Neuron. 65:550–562.

Andrews-Hanna JR, Snyder AZ, Vincent JL, Lustig C, Head D, Raichle ME, Buckner RL. 2007. Disruption of large-scale brain systems in advanced aging. Neuron. 56:924–935.

Barbas H, Ghashghaei H, Dombrowski SM, Rempel-Clower NL. 1999. Medial prefrontal cortices are unified by common connections with superior temporal cortices and distinguished by input from memory-related areas in the rhesus monkey. J Comp Neurol. 410:343–367.

Barber AD, Caffo BS, Pekar JJ, Mostofsky SH. 2013. Developmental changes in within- and between-network connectivity between late childhood and adulthood. Neuropsychologia. 51:156–167.

Bechara A, Damasio H, Tranel D, Damasio AR. 1997. Deciding advantageously before knowing the advantageous strategy. Science. 275:1293–1295.

Beckmann CF, DeLuca M, Devlin JT, Smith SM. 2005. Investigations into resting-state connectivity using independent component analysis. Philos Trans R Soc Lond B Biol Sci. 360:1001–1013.

Beltramini GC, Cendes F, Yasuda CL. 2015. The effects of antiepileptic drugs on cognitive functional magnetic resonance imaging. Quant Imaging Med Surg. 5:238–246.

Biswal B, Yetkin FZ, Haughton VM, Hyde JS. 1995. Functional connectivity in the motor cortex of resting human brain using echo-planar MRI. Magn Reson Med. 34:537–541.

Boes AD, Prasad S, Liu H, Liu Q, Pascual-Leone A, Caviness VS Jr, Fox MD. 2015. Network localization of neurological symptoms from focal brain lesions. Brain. 138:3061–3075.

Boveroux P, Vanhaudenhuyse A, Bruno MA, Noirhomme Q, Lauwick S, Luxen A, Degueldre C, Plenevaux A, Schnakers C, Phillips C,, et al. 2010. Breakdown of within- and between-network resting state functional magnetic resonance imaging

connectivity during propofol-induced loss of consciousness. Anesthesiology. 113:1038–1053.
Buckner RL, Andrews-Hanna JR, Schacter DL. 2008. The brain's default network: anatomy, function, and relevance to disease. Ann N Y Acad Sci. 1124:1–38.
Buckner RL, Krienen FM. 2013. The evolution of distributed association networks in the human brain. Trends Cogn Sci. 17:648–665.
Buckner RL, Sepulcre J, Talukdar T, Krienen FM, Liu H, Hedden T, Andrews-Hanna JR, Sperling RA, Johnson KA. 2009. Cortical hubs revealed by intrinsic functional connectivity: mapping, assessment of stability, and relation to Alzheimer's disease. J Neurosci. 29:1860–1873.
Bullmore E, Sporns O. 2009. Complex brain networks: graph theoretical analysis of structural and functional systems. Nat Rev Neurosci. 10:186–198.
Bullmore E, Sporns O. 2012. The economy of brain network organization. Nat Rev Neurosci. 13:336–349.
Carter AR, Astafiev SV, Lang CE, Connor LT, Rengachary J, Strube MJ, Pope DL, Shulman GL, Corbetta M. 2010. Resting interhemispheric functional magnetic resonance imaging connectivity predicts performance after stroke. Ann Neurol. 67:365–375.
Carter AR, Patel KR, Astafiev SV, Snyder AZ, Rengachary J, Strube MJ, Pope A, Shimony JS, Lang CE, Shulman GL,, et al. 2012. Upstream dysfunction of somatomotor functional connectivity after corticospinal damage in stroke. Neurorehabil Neural Repair. 26:7–19.
Chai XJ, Ofen N, Gabrieli JD, Whitfield-Gabrieli S. 2014. Selective development of anticorrelated networks in the intrinsic functional organization of the human brain. J Cogn Neurosci. 26:501–513.
Cole MW, Pathak S, Schneider W. 2010. Identifying the brain's most globally connected regions. Neuroimage. 49:3132–3148.
Corbetta M. 2012. Functional connectivity and neurological recovery. Dev Psychobiol. 54:239–253.
Dalley JW, Everitt BJ, Robbins TW. 2011. Impulsivity, compulsivity, and top-down cognitive control. Neuron. 69:680–694.
Damoiseaux JS, Rombouts SA, Barkhof F, Scheltens P, Stam CJ, Smith SM, Beckmann CF. 2006. Consistent resting-state networks across healthy subjects. Proc Natl Acad Sci USA. 103:13848–13853.
Devinsky O, Morrell MJ, Vogt BA. 1995. Contributions of anterior cingulate cortex to behaviour. Brain. 118(Pt 1):279–306.
Di X, Biswal BB. 2014. Identifying the default mode network structure using dynamic causal modeling on resting-state functional magnetic resonance imaging. Neuroimage. 86: 53–59.
Di Pino G, Pellegrino G, Assenza G, Capone F, Ferreri F, Formica D, Ranieri F, Tombini M, Ziemann U, Rothwell JC,, et al. 2014. Modulation of brain plasticity in stroke: a novel model for neurorehabilitation. Nat Rev Neurol. 10:597–608.
Eldaief MC, Halko MA, Buckner RL, Pascual-Leone A. 2011. Transcranial magnetic stimulation modulates the brain's intrinsic activity in a frequency-dependent manner. Proc Natl Acad Sci USA. 108:21229–21234.
Fellows LK. 2007. Advances in understanding ventromedial prefrontal function: the accountant joins the executive. Neurology. 68:991–995.
Ferreira LK, Regina AC, Kovacevic N, Martin MD, Santos PP, Carneiro CG, Kerr DS, Amaro E Jr, McIntosh AR, Busatto GF. 2015. Aging effects on whole-brain functional connectivity in adults free of cognitive and psychiatric disorders. Cereb Cortex. doi:10.1093/cercor/bhv190.
Fox MD, Greicius M. 2010. Clinical applications of resting state functional connectivity. Front Syst Neurosci. 4:19.
Fox MD, Snyder AZ, Vincent JL, Corbetta M, Van Essen DC, Raichle ME. 2005. The human brain is intrinsically organized into dynamic, anticorrelated functional networks. Proc Natl Acad Sci USA. 102:9673–9678.
Fox MD, Zhang D, Snyder AZ, Raichle ME. 2009. The global signal and observed anticorrelated resting state brain networks. J Neurophysiol. 101:3270–3283.
Fransson P, Marrelec G. 2008. The precuneus/posterior cingulate cortex plays a pivotal role in the default mode network: evidence from a partial correlation network analysis. Neuroimage. 42:1178–1184.
Frings L, Schulze-Bonhage A, Spreer J, Wagner K. 2009. Remote effects of hippocampal damage on default network connectivity in the human brain. J Neurol. 256:2021–2029.
Gao W, Zhu H, Giovanello KS, Smith JK, Shen D, Gilmore JH, Lin W. 2009. Evidence on the emergence of the brain's default network from 2-week-old to 2-year-old healthy pediatric subjects. Proc Natl Acad Sci USA. 106:6790–6795.
Gillebert CR, Mantini D. 2013. Functional connectivity in the normal and injured brain. Neuroscientist. 19:509–522.
Gratton C, Nomura EM, Perez F, D'Esposito M. 2012. Focal brain lesions to critical locations cause widespread disruption of the modular organization of the brain. J Cogn Neurosci. 24:1275–1285.
Hampson M, Driesen N, Roth JK, Gore JC, Constable RT. 2010. Functional connectivity between task-positive and task-negative brain areas and its relation to working memory performance. Magn Reson Imaging. 28:1051–1057.
Happaney K, Zelazo PD, Stuss DT. 2004. Development of orbitofrontal function: current themes and future directions. Brain Cogn. 55:1–10.
He BJ, Snyder AZ, Vincent JL, Epstein A, Shulman GL, Corbetta M. 2007. Breakdown of functional connectivity in frontoparietal networks underlies behavioral deficits in spatial neglect. Neuron. 53:905–918.
Heine L, Soddu A, Gomez F, Vanhaudenhuyse A, Tshibanda L, Thonnard M, Charland-Verville V, Kirsch M, Laureys S, Demertzi A. 2012. Resting state networks and consciousness: alterations of multiple resting state network connectivity in physiological, pharmacological, and pathological consciousness states. Front Psychol. 3:295.
Holmes AJ, Hollinshead MO, O'Keefe TM, Petrov VI, Fariello GR, Wald LL, Fischl B, Rosen BR, Mair RW, Roffman JL, et al. 2015. Brain Genomics Superstruct Project initial data release with structural, functional, and behavioral measures. Sci Data. 2:150031.
Honey CJ, Sporns O. 2008. Dynamical consequences of lesions in cortical networks. Hum Brain Mapp. 29:802–809.
Horovitz SG, Braun AR, Carr WS, Picchioni D, Balkin TJ, Fukunaga M, Duyn JH. 2009. Decoupling of the brain's default mode network during deep sleep. Proc Natl Acad Sci USA. 106:11376–11381.
Hutchison RM, Hashemi N, Gati JS, Menon RS, Everling S. 2015. Electrophysiological signatures of spontaneous BOLD fluctuations in macaque prefrontal cortex. Neuroimage. 113:257–267.
Hutchison RM, Morton JB. 2015. Tracking the brain's functional coupling dynamics over development. J Neurosci. 35:6849–6859.
Jilka SR, Scott G, Ham T, Pickering A, Bonnelle V, Braga RM, Leech R, Sharp DJ. 2014. Damage to the salience network and interactions with the default mode network. J Neurosci. 34:10798–10807.

Kaiser M, Martin R, Andras P, Young MP. 2007. Simulation of robustness against lesions of cortical networks. Eur J Neurosci. 25:3185–3192.

Keller CJ, Bickel S, Honey CJ, Groppe DM, Entz L, Craddock RC, Lado FA, Kelly C, Milham M, Mehta AD. 2013. Neurophysiological investigation of spontaneous correlated and anticorrelated fluctuations of the BOLD signal. J Neurosci. 33: 6333–6342.

Kelly AM, Uddin LQ, Biswal BB, Castellanos FX, Milham MP. 2008. Competition between functional brain networks mediates behavioral variability. Neuroimage. 39:527–537.

Kobayashi Y, Amaral DG. 2007. Macaque monkey retrosplenial cortex: III. Cortical efferents. J Comp Neurol. 502:810–833.

Leech R, Braga R, Sharp DJ. 2012. Echoes of the brain within the posterior cingulate cortex. J Neurosci. 32:215–222.

Liang X, He Y, Salmeron BJ, Gu H, Stein EA, Yang Y. 2015. Interactions between the salience and default-mode networks are disrupted in cocaine addiction. J Neurosci. 35:8081–8090.

Liang Z, King J, Zhang N. 2012. Anticorrelated resting-state functional connectivity in awake rat brain. Neuroimage. 59:1190–1199.

Lu J, Liu H, Zhang M, Wang D, Cao Y, Ma Q, Rong D, Wang X, Buckner RL, Li K. 2011. Focal pontine lesions provide evidence that intrinsic functional connectivity reflects polysynaptic anatomical pathways. J Neurosci. 31:15065–15071.

Mattfeld AT, Gabrieli JD, Biederman J, Spencer T, Brown A, Kotte A, Kagan E, Whitfield-Gabrieli S. 2014. Brain differences between persistent and remitted attention deficit hyperactivity disorder. Brain. 137:2423–2428.

Miao X, Wu X, Li R, Chen K, Yao L. 2011. Altered connectivity pattern of hubs in default-mode network with Alzheimer's disease: an Granger causality modeling approach. PLoS One. 6:e25546.

Mitchell JP, Banaji MR, Macrae CN. 2005. The link between social cognition and self-referential thought in the medial prefrontal cortex. J Cogn Neurosci. 17:1306–1315.

Muller-Oehring EM, Jung YC, Pfefferbaum A, Sullivan EV, Schulte T. 2015. The resting brain of alcoholics. Cereb Cortex. 25:4155–4168.

Murphy K, Birn RM, Handwerker DA, Jones TB, Bandettini PA. 2009. The impact of global signal regression on resting state correlations: are anti-correlated networks introduced? Neuroimage. 44:893–905.

Murphy TH, Corbett D. 2009. Plasticity during stroke recovery: from synapse to behaviour. Nat Rev Neurosci. 10:861–872.

Nomura EM, Gratton C, Visser RM, Kayser A, Perez F, D'Esposito M. 2010. Double dissociation of two cognitive control networks in patients with focal brain lesions. Proc Natl Acad Sci USA. 107:12017–12022.

Ovadia-Caro S, Villringer K, Fiebach J, Jungehulsing GJ, van der Meer E, Margulies DS, Villringer A. 2013. Longitudinal effects of lesions on functional networks after stroke. J Cereb Blood Flow Metab. 33:1279–1285.

Power JD, Cohen AL, Nelson SM, Wig GS, Barnes KA, Church JA, Vogel AC, Laumann TO, Miezin FM, Schlaggar BL,, et al. 2011. Functional network organization of the human brain. Neuron. 72:665–678.

Power JD, Schlaggar BL, Lessov-Schlaggar CN, Petersen SE. 2013. Evidence for hubs in human functional brain networks. Neuron. 79:798–813.

Rehme AK, Grefkes C. 2013. Cerebral network disorders after stroke: evidence from imaging-based connectivity analyses of active and resting brain states in humans. J Physiol. 591:17–31.

Scholvinck ML, Maier A, Ye FQ, Duyn JH, Leopold DA. 2010. Neural basis of global resting-state fMRI activity. Proc Natl Acad Sci USA. 107:10238–10243.

Sepulcre J, Liu H, Talukdar T, Martincorena I, Yeo BT, Buckner RL. 2010. The organization of local and distant functional connectivity in the human brain. PLoS Comput Biol. 6:e1000808.

Shehzad Z, Kelly AM, Reiss PT, Gee DG, Gotimer K, Uddin LQ, Lee SH, Margulies DS, Roy AK, Biswal BB,, et al. 2009. The resting brain: unconstrained yet reliable. Cereb Cortex. 19:2209–2229.

Silasi G, Murphy TH. 2014. Stroke and the connectome: how connectivity guides therapeutic intervention. Neuron. 83:1354–1368.

Smith SM, Miller KL, Moeller S, Xu J, Auerbach EJ, Woolrich MW, Beckmann CF, Jenkinson M, Andersson J, Glasser MF,, et al. 2012. Temporally-independent functional modes of spontaneous brain activity. Proc Natl Acad Sci USA. 109:3131–3136.

Sridharan D, Levitin DJ, Menon V. 2008. A critical role for the right fronto-insular cortex in switching between central-executive and default-mode networks. Proc Natl Acad Sci USA. 105: 12569–12574.

Stuss DT. 2011. Traumatic brain injury: relation to executive dysfunction and the frontal lobes. Curr Opin Neurol. 24:584–589.

Supekar K, Uddin LQ, Prater K, Amin H, Greicius MD, Menon V. 2010. Development of functional and structural connectivity within the default mode network in young children. Neuroimage. 52:290–301.

Tomasi D, Volkow ND. 2011. Functional connectivity hubs in the human brain. Neuroimage. 57:908–917.

Uddin LQ, Kelly AM, Biswal BB, Castellanos FX, Milham MP. 2009. Functional connectivity of default mode network components: correlation, anticorrelation, and causality. Hum Brain Mapp. 30:625–637.

Van Dijk KR, Hedden T, Venkataraman A, Evans KC, Lazar SW, Buckner RL. 2010. Intrinsic functional connectivity as a tool for human connectomics: theory, properties, and optimization. J Neurophysiol. 103:297–321.

Van Dijk KR, Sabuncu MR, Buckner RL. 2012. The influence of head motion on intrinsic functional connectivity MRI. Neuroimage. 59:431–438.

van Meer MP, van der Marel K, Wang K, Otte WM, El Bouazati S, Roeling TA, Viergever MA, Berkelbach van der Sprenkel JW, Dijkhuizen RM. 2010. Recovery of sensorimotor function after experimental stroke correlates with restoration of resting-state interhemispheric functional connectivity. J Neurosci. 30:3964–3972.

Vincent JL, Kahn I, Snyder AZ, Raichle ME, Buckner RL. 2008. Evidence for a frontoparietal control system revealed by intrinsic functional connectivity. J Neurophysiol. 100:3328–3342.

Wandschneider B, Stretton J, Sidhu M, Centeno M, Kozak LR, Symms M, Thompson PJ, Duncan JS, Koepp MJ. 2014. Levetiracetam reduces abnormal network activations in temporal lobe epilepsy. Neurology. 83:1508–1512.

Wang L, Yu C, Chen H, Qin W, He Y, Fan F, Zhang Y, Wang M, Li K, Zang Y,, et al. 2010. Dynamic functional reorganization of the motor execution network after stroke. Brain. 133:1224–1238.

Warren DE, Power JD, Bruss J, Denburg NL, Waldron EJ, Sun H, Petersen SE, Tranel D. 2014. Network measures predict neuropsychological outcome after brain injury. Proc Natl Acad Sci USA. 111:14247–14252.

Whitfield-Gabrieli S, Thermenos HW, Milanovic S, Tsuang MT, Faraone SV, McCarley RW, Shenton ME, Green AI, Nieto-Castanon A, LaViolette P,, et al. 2009. Hyperactivity and hyperconnectivity of the default network in schizophrenia and in

first-degree relatives of persons with schizophrenia. Proc Natl Acad Sci USA. 106:1279–1284.

Wichmann FA, Hill NJ. 2001. The psychometric function: II. Bootstrap-based confidence intervals and sampling. Percept Psychophys. 63:1314–1329.

Wu X, Yu X, Yao L, Li R. 2014. Bayesian network analysis revealed the connectivity difference of the default mode network from the resting-state to task-state. Front Comput Neurosci. 8:118.

Yang GJ, Murray JD, Repovs G, Cole MW, Savic A, Glasser MF, Pittenger C, Krystal JH, Wang XJ, Pearlson GD,, et al. 2014. Altered global brain signal in schizophrenia. Proc Natl Acad Sci USA. 111:7438–7443.

Yeo BT, Krienen FM, Chee MW, Buckner RL. 2013. Estimates of segregation and overlap of functional connectivity networks in the human cerebral cortex. Neuroimage. 88C: 212–227.

Yeo BT, Krienen FM, Eickhoff SB, Yaakub SN, Fox PT, Buckner RL, Asplund CL, Chee MW. 2015. Functional specialization and flexibility in human association cortex. Cereb Cortex. 25:3654–3672.

Yeo BT, Krienen FM, Sepulcre J, Sabuncu MR, Lashkari D, Hollinshead M, Roffman JL, Smoller JW, Zollei L, Polimeni JR,, et al. 2011. The organization of the human cerebral cortex estimated by intrinsic functional connectivity. J Neurophysiol. 106:1125–1165.

Yuan R, Di X, Taylor PA, Gohel S, Tsai YH, Biswal BB. 2016. Functional topography of the thalamocortical system in human. Brain Struct Funct. 221:1971–1984.